



PERFORMANCE CONTROL BASED ON GREEN TREE BEHAVIOR

M. Grigorian*

Mark Grigorian, MGA Structural Engineering Inc, Glendale, CA, USA

Received: 10 March 2014; **Accepted:** 25 June 2014

ABSTRACT

This article presents a realistic analogy, with practical applications, between green trees and manmade moment frames under similar loading conditions. The paper also introduces a new facet of bioinspiration which attempts to benefit from some of the natural design strategies involved in the structural performance of trees, rather than utilizing them as raw materials. The paper suggests that bioinspiration can help transfer and improve basic design concepts from trees to moment frames under seismic as well as gravity loading scenarios. For instance, it has been shown that earthquake resistant systems can best be realized by performing design led analysis rather than investigating analytic results and that structural design should be performance based rather than instruction oriented computations. In other words, it is preferable for earthquake resistant structures to be designed in accordance with observed rather than expected behavior, i.e., desirable response characteristics should be induced rather than investigated. These features constitute the core of the recently developed performance control (PC) methodology that aims at rational design of engineering structures under both service as well as extreme loading conditions. In the interim a number of new design formulae have also been introduced. Two examples have been provided to demonstrate the applications of the conceptual design similarities between green trees and earthquake resisting moment frames.

Keywords: Performance control; earthquake resistant; moment frames; trees; bioinspiration; lateral loading; uniform response; structural analogy.

NOTATION

F	magnification factor	H	total building height	U	internal energy
i, j	integer coordinates	I	beam moment of inertia	V	shear force
H	story height	J	col. moment of inertia	W	gravity load

*E-mail address of the corresponding author: markarjan@aom.com (M. Grigorian)

\bar{h}	height from base	K	subframe stiffness	G	weight
M	number of stories	L	span length	$\delta, \bar{\delta}$	displacement
N	number of bays	M	beam moment	Δ	displacement
S	order of occurrence	N	column moment	ϕ	drift ratio
C	numerical constant	P	gravity load	θ	virtual rotation
E	Elastic modulus	M^P	beam plastic moment	φ	imperfection
F	external force	N^P	column plastic moment	ψ	total drift

Indexes, superscripts and the secondary symbols are defined, as they first appear in the text.

1. INTRODUCTION

Architects and engineers have long known the benefits of bioinspiration for developing outstanding habitats and structures. Naturally evolved structures tend to result in truly optimal load bearing systems with respect to their function and environmental conditions, whereas the same cannot be generalised for manmade systems. Nature has developed many solutions to the problem of designing lateral resisting structures such as plants and trees. The characteristics of natural structures as listed in the literature are equally valid for all living entities including trees. However, a large number of organism-specific features have been identified which show that trees do act as natural frameworks [1-8].

A comparison of the current and emerging structural design concepts [9-12], shows that PC, [13-16], closely follows lessons learned from bioinspiration. A realistic, bioinspired design strategy that aims at reproducing observed response of any structure may appropriately be referred to as performance controlled rather than generically achieved. PC in this context implies the ability to design a structure in such a way as to expect predetermined modes of response, at certain stages of loading, extents of damage, and/or drift ratios.

The forthcoming parametric studies suggest that bioinspiration can help transfer basic design concepts from trees to simple moment frames under lateral and/or combined loading conditions. The process involving design methodology transfer from trees to moment frames, as expounded in this paper is achieved through four distinct but interrelated studies. In the Step 1 study, an attempt is made to identify and record the applicable characteristics of green trees that may be associated with the design and construction of moment frames. Some of the applicable characteristics of green trees, as perceived by the author and others are listed in the following section. The most pertinent characteristics of tree joints, roots, branches and the stem from a structural engineering point of view are presented in subsections 2.1 through 2.4. The in-depth study of the research findings of these steps leads to the establishment of the fundamental design principles presented under Section 3. These studies in turn lead to the proposed rules of methodology transfer from trees to manmade moment frames discussed as part of the Step 4 studies in subsections 4.1 and 4.2. The most important lesson learned from bioinspiration is that stresses and strains of green trees are optimized with respect to environmental conditions and tend to remain constant throughout the loading history of the structure. The phenomenon of uniform response as an important instrument of material optimization [19] is discussed in some

detail in the forthcoming sections. Design mimicry leads to the generation of idealized moment frames of uniform response (MFUR), [20-21] in which all beam ends develop the same level of elastic or plastic stresses without overstressing the adjoining columns. These idealized structures represent independent, fixed base moment frames, pin connected at the free ends of their branches, with the strength of the branches and the trunk increasing from the free to the fixed ends. Study Steps 5 and 6 consist of mathematical exercises that not only verify the validity and the coherence of the proposed manner of strategy transfer from tress to moment frames but also provide workable design examples for practical applications. Two exact, parametric examples are provided to illustrate the applications of the conceptual design similarities between trees and man made moment frames.

2. STRUCTURAL ATTRIBUTES OF GREEN TREES

All trees may be construed as cantilevered moment frames evolved to withstand various combinations of gravity and lateral forces. Trees are essentially three-dimensional, kinematically determinate systems that may be idealized as single degree of freedom objects for basic dynamic analysis. The results of these findings are then used to draw meaningful analogies between green trees and lateral resisting moment frames.

While there are countless numbers of natural characteristics that may be added to these lists, the present findings are selected to validate the strategic guidelines that form the basis of the recently developed performance control (PC) methodology for the efficient design of earthquake resisting moment frames.

2.1 Structural characteristics of tree trunks and branches

Some of the most applicable characteristics of green trees, from a structural engineering point of view that may be utilized in the design of earthquake resisting moment frames can be summarized as follows;

1. Trees are structures of uniform response, stresses and strains of all sections of its load bearing members are nearly the same under natural loading conditions.
2. Stresses due to self weight are minimal in comparison with snow and/or wind induced effects.
3. The cross sections of the stem and the branches are nearly symmetric. Torsional, local and global instability effects are minimized.
4. Branches and stems are structures of minimum weight. Each member is optimized for its own form and function.
5. The circular/oval cross-section of the branches and the trunks can withstand relatively greater compressive loads than any other solid cross section with the same amount of material. Circular cross sections can withstand relatively larger plastic moments of resistance than their equivalent rectangular sections. The shape factors for circular and rectangular sections are 1.7 and 1.5 respectively.

2.2 Structural materials of trees

The most relevant properties of materials of green tress can be enumerated as follows;

1. All members of a tree are made out of the same basic materials with varying strengths,

durabilities, toughness, thermal and elastic properties as required.

2. All trees are composed of purpose specific, direction oriented fibers.
3. All trees are made out of time tested, adaptable materials that can adjust themselves for changing environmental conditions.
4. Lack of mechanical ductility in trees is compensated by higher flexibility and damping.
5. Tree trunks and branches are naturally pre-stressed in both axial and circumferential directions.
6. Trees adjust their material strengths and composition in accordance with environmental requirements.

2.3 Structural characteristics of tree joints and connections

An understanding of the modes of response of loaded joints of green trees can help develop better earthquake resistant joints for practical moment frames.

1. Tree joints can achieve quasi-plastic response at extreme loading.
2. Tree roots are designed to be deformed and uplifted to a certain extent in order to prevent permanent damage to the base of the trunk.
3. Tree joints possess higher toughness than their connecting parts.
4. Tree joints are designed to fail and undergo large rotations without damaging the trunk.

2.4 Structural characteristics of trees as load bearing systems

The most applicable structural characteristics of green trees can be summarized as follows;

1. Trees are three dimensional, structurally determinate natural structures.
2. Trees can be classified as upright cantilevers and/or simple moment frames.
3. All tree members are singly connected cantilevered members, there are no simply supported or closed loop elements.
4. Trees can tolerate stresses due to initial out of straightness, local and global P-delta effects. (The P-delta moment which is the product of the total story level gravity force by the lateral displacement of the same story, tends to reduce the overall stiffness of the framing of that level and as such can lead to both local as well as global instabilities of the structure.)
5. Trees can sustain relatively large lateral displacements during extreme wind and snow conditions.
6. Trees are essentially multi-degree of freedom systems with high damping characteristics.

2.5 Trees as smart structures

Almost all trees adjust themselves for adapted environmental conditions and as such may be regarded as smart structures. Mattek [18] has noted that, “Trees optimize their mechanical design by adaptive growth, and react by self-repair to loads disturbing their optimum mechanical state.”

1. Trees are evolved (designed) following the laws of conservation of energy.
2. The leaves can orient themselves in such a way as to absorb/deflect sunlight, high winds, rain water and shed snow.
3. Trees orient their configuration in such a way as to avoid maximum external forces.
4. Mechanical strength is highly optimized with respect to local form and function.

5. Because of the multitude of independently vibrating elements and high damping properties, trees seldom experience resonant vibrations.
6. Trees are known to shed leaves and fruit, even mature branches in order to reduce P-delta effects and extreme stresses on the stem and the roots.
7. Trees grow on firm foundations with ample access to sunlight, moisture and nutrition.
8. Trees control and adjust their own performances through evolutionary processes.
9. All trees are environmentally friendly, energy efficient and recyclable structures.
10. In all trees framing patterns are highly repetitive.
11. In living trees failure and deterioration occur gradually, with the least important members failing first followed by the breakdown of the next important elements until no part of the system is stable.

2.6 Natural design strategies

While there are many differences between biology and structural engineering, this study concentrates mainly on the practical similarities that may help propose bio-inspired design strategies for certain types of manmade moment frames.

1. Trees appear to be formed in accordance with the rules of limit state stress distribution and minimization of external loading.
2. In green trees theories of structures and material science are embodied rather than followed.
3. Trees as natural structures are designed for functional (service) as well as survival (extreme) conditions. Function dictates the load paths and the stress-strain relationships in green trees.
4. Trees are generally symmetric in shape, with little to no eccentricity of the center of gravity. In green trees cross sections are as strong as needed. No part is stronger than needed.
5. Constitutive elements of trees are either repairable or can be compensated for.
6. The configurations and strength of trees are optimized with respect to their functions.
7. The total amount of energy expended to build and maintain a green tree is a minimum with respect to its function and environmental conditions.
8. The effects of out of plumbness in trees are compensated for by a combination of shifting of the C.G. of the tree and the additional resistance of the affected sections.
9. In the creation of trees, design and construction are not independently organized. In nature, planning and implementation are accomplished simultaneously.

3. DESIGN-RESPONSE ANALOGY

Results of several investigations, [5, 17-18], including the current research, point towards near perfect analogy between the evolutionary development of green trees and the laws governing the efficient design of earthquake resisting moment frames. A study of these results not only leads to the formulation of rational guidelines for the planning of efficient moment frames, but also verifies the validity of some of the existing rules of general application. Since the proven performance of trees can be assessed in terms of known principles of material science and applied mechanics, then their adaptive strategies for

survival can be utilized as ideal guidelines for planning man made moment frames. It is therefore reasonable to try to transfer structural design knowledge from living trees to engineering frameworks.

3.1 Strategic guidelines for selecting natural design strategies

The purpose of this section is to introduce a new facet of bioinspiration which attempts to unravel the natural design strategies involved in the structural performance of trees, rather than synthesizing new load bearing forms, substances and/or utilizing them as raw materials. And in doing so, the following guidelines come to mind;

- Develop a feel for the response of the real structure under all functional conditions.
- The laws of conservation of energy should be observed as the fundamental guidelines for the conceptual design of the moment frame under consideration.
- Theories of design and construction should be applied rather than followed.
- The fundamental idea expounded here is that the response of moment frames should be a function of design and construction rather than analysis.
- Planning should be based on design led analysis rather than analysis for design.
- Structural design should be performance based rather than instruction oriented. In other words, structures should be designed in accordance with observed rather than expected behavior.
- Desirable response characteristics should be provided for (induced) rather than investigated.
- It is constructive to induce and/or apply the desirable design conditions to the proposed moment frame rather than checking the analytic results for compliance against prescribed criteria.
- Minimize the self weight of all load bearing elements with respect to governing loading conditions.

3.2 Technical considerations for practical design applications

While the real life performance of trees can be looked upon as useful guidelines for engineers, the established principles of structural mechanics should also be taken into consideration for practical design purposes.

- Preferably, moment frames should be constructed out of similar members and materials.
- In a progressive collapse scenario, the premature failure of the base or foundation of the structure should be avoided at all cost.
- Develop a design strategy that is based on observed performance rather than expected response. Begin with planning a firm foundation for the proposed structure.
- Generate a statically determinate or quasi-determinate structure of uniform response for combined gravity and lateral loading. Lateral loads are known to generate constant drift ratios along the heights of moment frames of uniform response.
- Arrange the constituent materials /elements of the system in such a way as to maximize their stiffness and to lower their centre of gravity.

- Allow for material and geometric imperfections.
- Reduce dynamic effects by increasing the fundamental period of vibration. Provide as much damping as possible.
- Induce uniform drift in order to minimize secondary and instability effects.
- Allow for service and extreme functional displacements throughout the loading history of the structure.
- Prevent catastrophic failure through increased ductility, local and global stability as well as installation of fail-safe devices, etc.
- Allow for preplanned sequences of formations of plastic hinges at all beam ends.
- Implement the strong-column weak-beam principle and prevent and/or delay the premature formation of plastic hinges at column feet.
- Constitutive elements of structures shall be repairable, environmentally friendly and recyclable.

Both the strategic as well as technical considerations discussed above can be brought together as the conditions of analogy presented below.

3.3 System and member analogy

In order to utilize the functional and technical relationships that exist between green trees and moment frames, both the inspired as well as the established principles of science should be coalesced in favor of safe and economic solutions. Therefore, in order to capture and transfer design knowledge from trees to moment frames, the following basic rules of analogy should be taken into consideration:

- Structural similarities: i.e. the kinematics, geometry and the framing type of the model and the prototype should be closely similar, the distribution, use and behavior of materials should be similar in both systems.
- Functional similarities: i.e. both the model and the prototype are to withstand similar loading and environmental conditions.
- Response analogy: i.e. both the model and the prototype are expected to achieve the same response objectives against comparable service and extreme loading conditions.
- Economic viability: i.e. the bioinspired design should be more cost effective than its classical counterparts

3.4 Member equivalency

System equivalency may be achieved if the constitutive members of the moment frame, i.e. the beams, connections, columns and the supports can be simulated to perform much the same way as their counterparts in trees, i.e. the branches, the joints, the stem and the roots respectively of the prototype. Member equivalency and its extension, weight equivalency, are simple conceptual tools that have been devised to compare the bending of naturally occurring cantilevers to single span beams with different boundary conditions. Member equivalency is best introduced by way of the following example, where a straight fix ended

beam under uniform load q , Fig. 1(a), is assumed to be equivalent in nature to two cantilevers with similar or varying cross sections under similar loading.

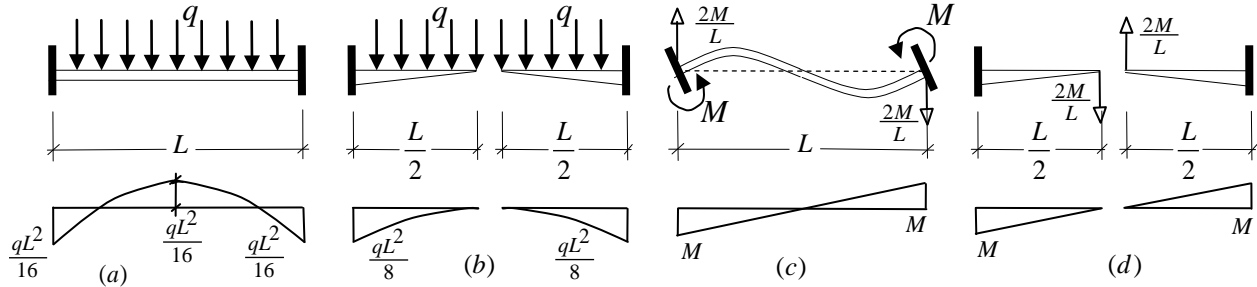


Figure 1. (a) Fix ended beam under uniform loading, (b) Twin equivalent, weight improved cantilevered beams under uniform loading, (c) Fixed beam under equal end moments, (d) Twin, equivalent, weight improved cantilevered beams under concentrated end loads.

It can be assumed that for any flexural element of uniform cross section such as that shown in Fig.1 (a), the total self weight can be computed as [1]:

$$G_a = \gamma L M_a^P \quad (1)$$

where suffixes a , b etc. refer to beams a , b etc. respectively, and γ is a constant of proportionality. Hence, for any flexural element of tapering section, such as that shown in Fig. 1(b), the weight per unit length may be related to the moment of resistance of that section, then the total self weight of the equivalent beams of variable section can be estimated, to a good degree of approximation, as:

$$G_b = 2\gamma \int_0^{\frac{L}{2}} M_b^P(x) dx \quad (2)$$

where, $M_b^P(x)$ is the plastic moment of resistance of section x of the element. Equations (1) and (2) may be utilized to show that for any single span beam of uniform section, e.g., Figs. 1(a) and 1(c), there can exist twin, reduced weight, cantilevers of variable sections such as Figs. 1(b) and 1(d) respectively, where the total weight of the modified systems are always less than or equal to that of the original member, i.e.:

$$G_b \leq G_a \text{ and } G_d \leq G_c \quad (3)$$

$$\text{Where, } G_a = \gamma M_a^P L = \frac{\gamma q L^3}{16} \text{ and } G_b = 2\gamma \int_0^{\frac{L}{2}} M_b(x) dx = 2\gamma \int_0^{\frac{L}{2}} \left[\frac{qx^2}{2} \right] dx = \frac{\gamma q L^3}{24} \quad (4)$$

$$G_c = \gamma M_c^P L \text{ and } G_d = 2\gamma \int_0^{\frac{L}{2}} M_d(x) dx = 2\gamma \int_0^{\frac{L}{2}} \left[\frac{2Mx}{L} \right] dx = \frac{\gamma M_d^P L^2}{2} \quad (5)$$

Similar arguments can be presented for other practical loading and boundary support conditions such as those depicted in Appendix 1. However, for the sake of brevity the scope of the current article has been limited to equivalent elements of uniform cross section only.

Performance control, as a structural design methodology is the most applicable feature of

bioinspiration adopted in this article. In the realms of structural analysis PC implies the imposition of desirable observed behavior rather than searching for suitable results, and as such it is based upon the fulfillment and/or implementation of the following design conditions that:

The selected configuration is suitable for the proposed functions. i.e., there are no significant irregularities. However, the effects of geometric and material imperfections can be incorporated as part of the general design strategy.

A moment frame of uniform response MFUR with constant drift angle can be generated. MFUR lend themselves well to demand-capacity adjustments during all phases of the loading. The basic rules governing the generation of MFUR are developed under sections 5.1 and 5.2 below.

The sequences of formations of the plastic hinges can be controlled in such a way as to meet target displacements and/or reduce stiffness degradation as required. Several commonly available technologies including reduced beam sections (RBS), added flange plates (AFP), etc., can be used to regulate the sequences of formations of plastic hinges in MFUR.

The strong column weak beam condition can be imposed throughout the frame, i.e. no soft story failure can take place.

The premature formation of plastic hinges at column feet can be prevented. This can enhance the displacement development potential of the system.

Target displacements at specified load levels shall not be exceeded.

In this particular context PC is the structural methodology that aims at rational transfer of design technologies from trees to moment frames under both service, i.e., elastic, as well as extreme loading, i.e. incipient collapse conditions. Results of inelastic static, push-over and dynamic time-history analyses [11] have shown that Performance Based Plastic Design methods can successfully be applied to almost all types of code recognized earthquake resisting systems. The phenomenon of uniform response as an important contribution of biomimetics is discussed in some detail in the forthcoming sections.

5. GENERATION OF MOMENT FRAMES OF UNIFORM RESPONSE

The next step in mimicking a design strategy from green trees is to generate a MFUR in which all beam ends develop the same level of elastic or plastic stresses without overstressing the adjoining columns. Any MFUR designed by the provisions of Section 4.2 can also serve as an envelope of several initial designs within which member sizes could be adjusted and/or modified for any purpose while observing the prescribed performance conditions. However, for practical member sizing purposes, only the study of two essential modes of response of MFUR, with initial imperfections, at first yield and at incipient collapse is warranted. The most important attributes of MFUR can be summarized as;

- MFUR represent minimum-weight design envelopes within which member sizes can be rearranged in such a way as to optimize material and construction costs without violating the prescribed member selection conditions.
- MFUR are ideally suited to performance control where target displacements can be related to any loading stage, including incipient collapse.

- In MFUR selected groups of beams and columns share the same drift and demand-capacity ratios.
- The ratio of total internal energy of any of MFUR to that of anyone of its levels, such as the roof, is equal to the ratio of the global overturning moment to the overturning moment of that (roof) Level.
- The ratio of stiffness of any two floors of a MFUR is proportional to the ratio of shear forces of the two levels multiplied by the inverse ratios of their heights [14, 15, 20, 21].
- All MFUR may be treated as statically determinate, SDOF structures.

5.1 Conceptual considerations

It is instructive to note that while small floor loads, i.e. $q_{small} \leq 4M^P / L^2$, have no effects on the lateral carrying capacity of the system, axial loads P tend to reduce its efficiency linearly from full capacity to zero at $P / P_{cr} = 1$, [14, 22]. Furthermore, comparing q_{small} with $q_{ultimate} = 4M^P / L^2$, it may be concluded that in general $q_{small} \leq q_{ultimate} / 2$. In other words, the magnitude of a uniformly distributed load may be considered small if it is less than half of its plastic collapse value acting alone on the same beam. Therefore, it may be concluded that moderate to small gravity loads have little to no effect on the drift and ultimate carrying capacity of earthquake resisting moment frames, which are designed for code level earthquakes. Expectedly, the locations of the imaginary hinges of Fig. 2(b) coincide with the points of inflexions of the beams of the prototype under lateral bending. The physical implications of these hinges together with the geometric requirements of the uniform drift move the locations of zero moments of the columns towards their mid height. These considerations reduce the otherwise complicated task of structural optimization to direct design through rational member selection and observation of recommended rules of application. The elastic and plastic performances of generalized MFUR are studied independently under Sections 5.2 and 5.3 respectively.

5.2 Basic linear analysis

The general scheme of a representative subframe of uniform response with initial imperfection $\bar{\delta}_i = \phi_i h_i$ under lateral shear force V_i and total accumulated axial nodal load $P_{i,j}$ is depicted in Fig. 3(a) below. The conceptual considerations described under 5.1 above allow the drift ratio of a typical subframe, Fig. 3a, without due consideration to ϕ_i and P-delta effects, be expressed as [20];

$$\phi_i = \frac{1}{12E} \left[\frac{V_i h_i}{\sum_{j=0}^n J_{i,j} / h_i} + \frac{V_i h_i + V_{i+1} h_{i+1}}{\sum_{j=1}^n \bar{I}_{i,j} / L_j} \right] \quad (6)$$

The subject moment frame is a structure of uniform response, therefore groups of its members with similar features such as beams and columns of the same bay will be forced to share the same demand-capacity ratios regardless of their location within the system, and as

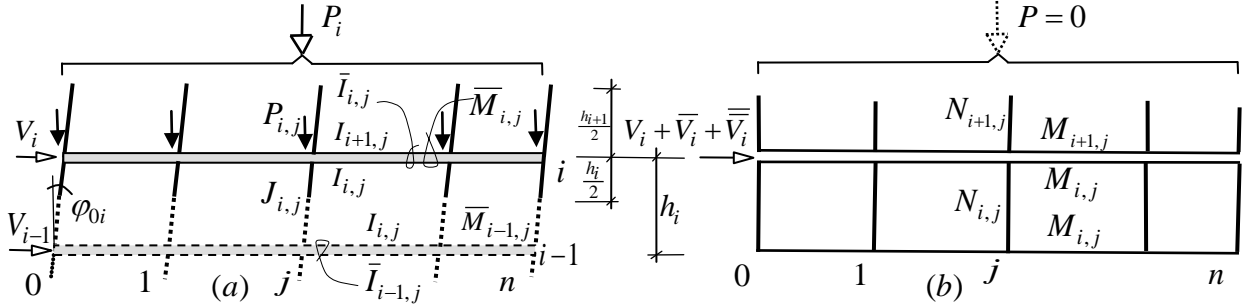


Fig. 3. (a) Laterally loaded subframe of uniform response with initial out of straightness, (b) Simplified straight model with zero gravity loading under notional lateral forces.

such the rule of proportionality, [20], requires that if $\bar{I}_{i,j} = I_{i,j} + I_{i+1,j}$ and $\bar{M}_{i,j} = M_{i,j} + M_{i+1,j}$ then,

$$\frac{V_i h_i + V_{i+1} h_{i+1}}{\sum_{j=1}^n \bar{I}_{i,j} / L_j} = \frac{V_i h_i}{2 \sum_{j=1}^n I_{i,j} / L_j} \quad (7)$$

Note that while $\bar{I}_{i,j}$ represents the moment of inertia of beam ij of the subframe of Fig. 3(a), $I_{i,j}$ stands for the proportion of $\bar{I}_{i,j}$ contributed by the upper beam of the imaginary subframe of Fig. 3(b). Equation (7) may now be used to simplify Equation (6) as:

$$\phi_i = \frac{\delta_i}{h_i} = \frac{V_i h_i}{12E} \left[\frac{1}{\sum_{j=0}^n \bar{k}_{i,j}} + \frac{1}{2 \sum_{j=1}^n k_{i,j}} \right] = \frac{V_i}{K_i h_i} \quad (8)$$

which describes the response of the simplified subframe under the same loading conditions as the prototype? Here, V_i , $k_{i,j} = \bar{I}_{i,j} / L_{i,j}$ and $\bar{k}_{i,j} = J_{i,j} / h_{i,j}$ are the story level shear force, beam and column relative stiffnesses respectively. Equations (6) and (8) are associated with Figs. 3(a) and 3(b) respectively and yield the same inter story drift ratios ϕ_i . However, Equation (8) lends itself better to the inclusion of initial imperfections as well as the P-delta effects. For a more comprehensive discussion of this topic the interested reader is referred to [23- 26].

5.2.1 Development of equivalent notional loading

While Fig. 3(a) depicts an imperfect subframe under lateral and axial loading, Fig. 3(b) represents its equivalent perfect counterpart under notional shear forces \bar{V}_i and \bar{V}_i with zero axial loads. Supposing the effects of the axial joint forces and the initial imperfections ϕ_{0i} could be studied through the following equivalent/notional force equations:

$$\sum_{j=0}^n P_{i,j} \delta_i = \bar{V}_i h_i \quad \text{and} \quad \sum_{j=0}^n P_{i,j} h_i \phi_i = \bar{V}_i h_i \quad (9)$$

or $\bar{V}_i = P_i \delta_i / h_i$ and $\bar{\bar{V}}_i = P_i \varphi_{0i}$ respectively, where $P_i = \sum_{j=0}^n P_{i,j}$ is the total gravity load acting on i level, then Equation (8) may be expanded to include the additional effects of \bar{V}_i and $\bar{\bar{V}}_i$, i.e.

$$\Delta_i = \frac{V_i}{K_i} + \frac{\bar{V}_i}{K_i} + \frac{\bar{\bar{V}}_i}{K_i} \quad \text{or} \quad \Delta_i = \frac{V_i}{(1-\mu_i)K_i} + \frac{\mu_i \bar{\delta}_i}{(1-\mu_i)} = \frac{V_i + P_i \varphi_{0i}}{(1-\mu_i)K_i} \quad (10)$$

where $\mu_i = P_i / K_i h_i$ and $f_{cr,i} = (1-\mu_i)$ are commonly referred to as the corresponding stability quotient and the load magnifying factors respectively. Simply stated the magnitude of the effective shear acting on the perfectly straight model with zero axial loading may be computed as:

$$V_i + \bar{V}_i + \bar{\bar{V}}_i = \frac{V_i + P_i \varphi_{0i}}{(1-\mu_i)K_i} \quad (11)$$

If the original moment of resistance of the system with $P_i = \varphi_{0i} = 0$ is symbolized by \mathbf{M} , $= V_i h$ then it would reduce to $V_i h_i (1-\mu_i) - \varphi_{0i} h_i P_i = (1-\mu_i) \mathbf{M} - P \Delta_0$. If $\Delta_i = \delta_i + \bar{\delta}_i$ and $\delta_i = V_i / K_i$ denote the total lateral displacements of the structure with and without the combined P-delta and out of straightness effects respectively, then it may be shown, Appendix 2, Equation B (2), that:

$$\Delta_i = \frac{\delta_i + \bar{\delta}_i}{(1-\mu_i)} \quad \text{and} \quad \psi_i = \frac{\phi_i + \varphi_{0i}}{(1-\mu_i)} \quad (12)$$

where ψ_i is the total drift ratio due to all causes including the initial imperfections. The novelty of Equations (11) and (12) is in that they can allow for variations of φ_{0i} along the height of the structure. The required stiffness for any such subframe may now be expressed, Equation B (3), as:

$$K_i = \frac{V_i + \psi_i P_i}{(\psi_i - \varphi_{0i}) h_i} \quad (13)$$

The significance of Equation (13) is in that it not only directly relates the P-delta effects and the initial imperfections to the target displacements and the desired total stiffness, prior to making an attempt at numerical analysis, but also provides a direct means of controlling the corresponding load reduction or stability function in terms of the initial and final geometric parameters, i.e.:

$$f_{cr,i} = (1-\mu_i) = 1 - \frac{P_i}{K_i h_i} = 1 - \left[\frac{P_i \psi_i - P_i \varphi_{0i}}{P_i \psi_i + V_i} \right] \quad (14)$$

It has been reported [27, 28] that uniform drift can help improve racking stability in all categories of moment frames. A consideration of the equilibrium equation of the subject subframe in terms of its internal moments $M_{i,j}$ and $N_{i,j}$ acting at the joints i and j of beams and columns respectively, gives:

$$M_{i,j} = \frac{(V_i + P_i \phi_{0i}) h_i k_{i,j}}{4(1 - \mu_i) \sum_{j=1}^n k_{i,j}} \quad \text{and} \quad N_{i,j} = \frac{(V_i + P_i \phi_{0i}) h_i \bar{k}_{i,j}}{2(1 - \mu_i) \sum_{j=0}^n \bar{k}_{i,j}} \quad (15)$$

The difference between ψ_i and ψ_{i+1} is known as the drift shift [28] and can be minimized or reduced to zero by imposing a uniform inter story drift $\psi_i = \psi_{i+1} = \psi_m = \phi$ along the height of the structure. If the structure is of uniform response and ϕ is known, then the following general laws of proportionality may be employed to assure uniform drift along the height of the frame:

$$\sum_{j=0}^n \bar{k}_{i,j} = \left[\frac{V_i K_i h_i^2}{V_m K_m h_m^2} \right] \sum_{j=0}^n \bar{k}_{m,j} \quad \text{and} \quad \sum_{j=1}^n k_{i,j} = \left[\frac{V_i K_i h_i^2}{V_m K_m h_m^2} \right] \sum_{j=1}^n k_{m,j} \quad (16)$$

If $I_{i,j}$ and $J_{i,j}$ are selected in accordance with the requirements of Equations (16), then the subject structure can be classified as a MFUR, and as such the corresponding solutions may be considered as exact and unique [29,30].

5.2.3 Modeling and member selection strategies

While there are several options for the preliminary selection of the beams and columns of any MFUR, certain alternatives [14] appear to be better suited for performance control, strategic decision making as well as mathematical modeling. A study of Equations (8)-(15) reveals that subframe stiffness K_i and its components $\sum_{j=0}^n \bar{k}_{i,j}$ and $\sum_{j=1}^n k_{i,j}$ are independent of the positions of its members along the length of the frame during all phases of the degradation process or loss of stiffness of the structure. This implies that the members of the mathematical model can be arranged in such a way as to simplify the corresponding sequential computations and provide insight into the behavior of the structure throughout the loading history of the system starting from zero to first yield and from first yield to incipient collapse. In developing the mathematical formulae of Section 5.2 an observation was made that the redistribution of moments through formation of plastic hinges at the ends of the beams forces the corresponding points of inflexion to move to mid span, whence the corroborating assumption that points of inflexions of all beams also occur at their mid spans during the initial elastic stages as well as plastic modes of response. This is an excellent assumption with inconsequential margins of error since the solution becomes more accurate and eventually exact as plasticity spreads over the remaining members of the structure.

Since efficient MFUR are designed, to fail through global, kinematically acceptable, [31-32], sway mechanisms involving beam end plastic hinges only, then a well arranged model would lend itself to a more insightful study of the sequences of simultaneous failures of the

beams of the bays, rather than the order of formation of individual plastic hinges. For instance, if the beams of constant cross section of the prototype are specified as $L_1 = 1.5L$, $L_2 = 2L$ and $L_3 = L$, then the spans of the model, as in Fig. 4a would best be arranged in the descending order of the stiffnesses of the individual beams, i.e., $L_1 = L$, $L_2 = 1.5L$ and $L_3 = 2L$.

5.2.4 Introductory example 1, generation of a MFUR with initial imperfections

Generate an $m \times n = 4 \times 3$ MFUR corresponding to Fig. 4a, under lateral forces $F_i = F\bar{h}_i / H$, nodal axial forces $p_{i,j} = p$ and initial imperfection $\phi_{0i} = 0.0025$ radians. Compute the lateral shear force F_Y at first yield in such a way as not to exceed the target drift ratio $\phi_Y \leq 0.01$ radians. Assume $p = 2F$ and use beams of constant cross sections for all levels such that $I_{i,j} = I_i$, $M_{i,j}^P = M_i^P$, $J_{i,j} = J_i$. Use; $J_{i,0} = J_{i,3} = J_i$ and $N_{i,0}^P = N_{i,3}^P = \lambda M_i^P$, and $J_{i,1} = J_{i,2} = 2J_i$ and $N_{i,1}^P = N_{i,2}^P = 2\lambda M_i^P$ for the exterior and interior columns respectively. $h = L$, $I = J$ and $\lambda > 1$. Here λ is the code required over strength factor.

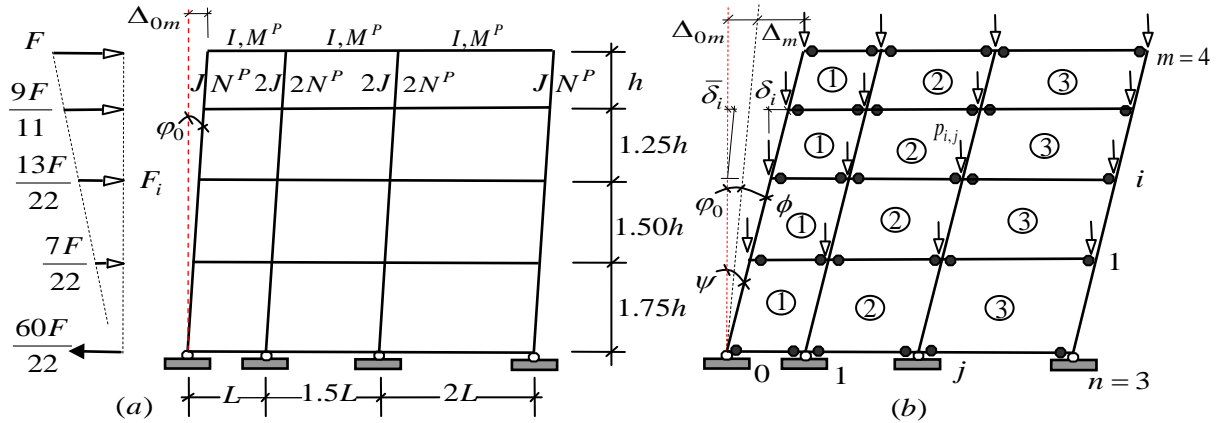


Figure 4. (a) Geometry and loading, (b) Collapse mode & sequence of failures of bays

Solution: Select the properties of the members of the uppermost subframe as; $I_m = I$, $M_m^P = M^P$, $J_{m,0} = J_{m,3} = J$, $J_{m,1} = J_{m,2} = 2J$, $N_{m,0}^P = N_{m,3}^P = \lambda M^P$ and $N_{m,1}^P = N_{m,2}^P = 2\lambda M^P$ for level m . It follows that; $\bar{k}_{4,0} = \bar{k}_{4,3} = J/h$, $\bar{k}_{4,1} = \bar{k}_{4,2} = 2J/h$, $k_{4,1} = I/L$, $k_{4,2} = 2I/3L$, $k_{4,3} = I/2L$,

$$P_4 = \sum_{j=0}^{n=3} p_{4,j} = 4p = 8F, \quad \sum_{j=0}^{n=3} \bar{k}_{4,j} = 6J/h, \quad \sum_{j=1}^{n=3} k_{4,j} = 13I/6L. \quad \text{Equations (8) and (13) give;}$$

$$\frac{1}{K_4} = \frac{h^2}{12E} \left[\frac{h}{6J} + \frac{6L}{2 \times 13I} \right] = \frac{31h^3}{936EI} \quad \text{and} \quad K_4 = \frac{V_4 + \phi_Y P_4}{(\phi_{T,4} - \phi_4)h_4} = \frac{(F + .01 \times 8F)}{(0.01 - .0025)h} = \frac{144F}{h} \text{ respectively.}$$

See Appendix 3. The elimination of K_4 establishes $I = I_Y = 4.7692Fh^2/E$. The load reduction factor

$$\text{For the roof level subframe may now be computed as;}$$

$$f_{cr,4} = (1 - \mu_i) = 1 - \frac{P_4}{K_4 h_4} = 1 - \frac{8Fh}{144Fh} = \frac{17}{18}.$$

Obviously since the beams of bay number 1 are stiffer than the corresponding beams of the other two bays, first yield occurs at the ends of the former set of beams, whence Equation (15), Appendix 4 gives, $M_{4,1} = M_m^P = M^P = 0.1319Fh$, $M_{4,2} = 0.0879Fh = 2M^P/3$ and $M_{4,3} = 0.0659Fh = M^P/2$.

Therefore $F = F_Y = 7.5815M^P/h$. The complete parametric solution of Example 1 is presented in Table 1 below. The results of this table indicate that the most important utility of PC is its ability to control the magnitude and distribution of moments with respect to predetermined force levels and stipulated drift angles. In other words the quantities I and J can be computed in such a way as to maintain a uniform drift along the height of the frame. The drift profile in Fig. 4b is a straight line.

Table 1: Numerical solution of Example 1 MFUR with $\phi_0 = 0.0025$, $\phi_Y = 0.01$ and $I = 4.7692Fh^2/E$

i	F_i/F	V_i/F	h_i	$V_i h_i / Fh$	$K_i/(h/F)$	$f_{cr,i}$	I_i/I	\bar{I}_i/I	$M_{i,1}/Fh$	$\bar{M}_{i,1}/Fh$
4	1.0000	1.0000	1.00	1.0000	144.00	00.9444	1.0000	1.01.0000	10.1319	0.1319
3	0.8182	1.8182	1.25	2.2728	211.00	00.9393	22.5298	3.5298	0.2430	0.3740
2	0.5909	2.4091	1.50	3.6137	235.48	00.9321	44.4509	6.9809	0.3279	0.5709
1	0.3182	2.7273	1.75	4.7728	232.18	00.9212	66.4909	10.9418	0.3817	0.7096
0	2.7273	-	5.50	11.6593	-	-	-	46.4909	-	0.3817

6. ULTIMATE LIMIT STSATE ANALYSIS

The mathematical nature of Equations (8), (11) and (13) suggest that the second order behavior of the subject subframes can be incorporated as part of any stepwise first order analysis by means of equivalent notional force modeling, where the notional forces are assumed to act concurrently with the applied lateral forces on a perfectly straight model with no axial loading. Here, the idea has been further developed to establish a simple elastic-plastic procedure that reduces the task of otherwise complicated nonlinear computations to direct formulation of the elastoplastic response of imaginary subframes as constituent parts of the MFUR.

If the analysis of an imperfect or skewed MFUR subjected to global P-delta effects is compared to that of a theoretically equivalent straight frame free of axial forces, it may be seen that there are certain similarities between the analytic stages of the two systems. The inherent likenesses between the prototype and equivalent model always lead to the same results. Here, the equivalent notional force concept has been utilized as the progenitor of progressive simultaneous group failure modeling, where the notional capacities are treated as the inherent property of the equivalent frame with zero P-delta effects.

6.1 The stepwise approach

Consider the preferred progressive group failure pattern of Fig. 4b under factored lateral forces F_i , initial imperfection ϕ_0 and nodal axial loads $p_{i,j}$. If the plastic moments of resistance of the beams and columns of the frame are denoted by $M_{i,j}^P$ and $N_{i,j}^P$ respectively,

where by the requirements of the strong column-weak beam principle $(N_{i,j}^P + N_{i+1,j}^P) \geq \lambda(M_{i,j}^P + M_{i,j+1}^P)$ and $\lambda > 1$ is the column over-strength factor, then the plastic bending moments required to generate first yield at the ends of the beams of the first bay or identical bays of the uppermost imaginary subframe, $i = m$, may be computed as:

$$M_{m,1} = \frac{(V_m + P_m \varphi_{0m}) h_m k_{m,1}}{4(1 - \mu_m) \sum_{j=1}^n k_{m,j}} = M^P \text{ and } M_{m,j} = \left(\frac{k_{m,j}}{k_{m,1}} \right) M^P \text{ for } j = 1, 2, \dots, n \quad (17)$$

The terms $P_m \varphi_{0m}$ and μ_m describe the effects of initial imperfections and the global P-delta phenomenon on the elastoplastic response of the selected subframe. Now, if there are $r \leq n$ distinct loading stages identified by the subscript $s = 1, 2, \dots, r$ and $1 \leq \tau_{m,s} \leq r$ is the number of simultaneously failing bays at stage s , then the magnitude of the total lateral force needed to generate first yield (plastic hinges at the ends of the beams of bay number 1) at the culmination of phase one loading can be estimated as:

$$(V_{m,s=1} + P_{m,s=1} \delta_s^1 \varphi_{0m}) = \frac{4\tau_{m,s=1} M^P}{k_{m,1} h_m} (1 - \mu_{m,s=1}) \sum_{r=s=1}^n k_{m,r} \quad (18)$$

Where, $\delta_s^1 = 1$ for $s=1$ and $\delta_s^1 = 0$ for $s>1$ has been introduced to limit the effects of initial out of straightness to the nonlinear response of the system within the elastic range. Next, bearing in mind that the sequence of formation of the plastic hinges of any level is the same as the descending order of the stiffnesses of the beams of the same floor, then the effective moment induced in the remaining elements of the subframe at the end of phase one loading can be computed by Equation (17) as $(k_{m,j} / k_{m,1})(1 - \mu_1) M^P$. Therefore the balance of bending moments needed to elevate the moments of resistance of the beams of the next bay or bays to M^P can be computed as $[(1 - \mu_2) - (1 - \mu_1)(k_{m,2} / k_{m,1})] M^P$, whence the amount of additional force required to generate plastic hinges at the ends of the beams of the next stiffest bay or bays can be expressed as;

$$V_{m,s=2} = \frac{4M^P}{k_{m,s=2} h_m} \left[\tau_{m,s=2} (1 - \mu_{m,s=2}) - \tau_{m,s=1} (1 - \mu_{m,s=1}) \left(\frac{k_{m,s=2}}{k_{m,s=1}} \right) \right] \sum_{j=s}^n k_{m,j} \quad (19)$$

Or in its most generalized form as:

$$V_{m,s} + P \delta_s^1 \varphi_{0m} = \frac{4M^P}{h_m} \left[\frac{\tau_{m,s} (1 - \mu_{m,s})}{k_{m,s}} - \frac{\tau_{m,s-1} (1 - \mu_{m,s-1})}{k_{m,s-1}} \right] \sum_{j=s}^n k_{m,j} = \frac{4M^P}{h_m} \alpha(m, s) \quad (20)$$

Similarly, the corresponding incremental displacement may be expressed as:

$$\Delta_{m,s} = \frac{V_{m,s} + P\delta_s^1\phi_{0m}}{(1-\mu_{m,s})K_{m,s}} = \frac{4M^P\alpha(m,s)}{(1-\mu_{m,s})K_{m,s}h_m} \quad (21)$$

Here function $\alpha(m,s)$ has been introduced for brevity of text only. However, if there are $r \leq n$ distinct loading stages then the total lateral force, V_m^P needed to cause plastic failure of the subframe can be computed as:

$$V_P + P\phi_{0m} = \sum_{s=1}^r (V_{m,s} + P\delta_s^1\phi_{0m}) = \frac{4M^P}{h_m} \sum_{s=1}^r \alpha(m,s) = \frac{4M^P}{h_m} \sum_{s=1}^r (1-\mu_{m,s}) \quad (22)$$

And the corresponding total lateral displacement at incipient collapse with respect to its base as:

$$\Delta_m^P = \sum_{s=1}^r \Delta_{m,s} = \frac{4M^P}{h_m} \sum_{s=1}^r \frac{\alpha(m,s)}{(1-\mu_{m,s})K_{m,s}} \quad (23)$$

If $P_m = \phi_{0m} = \mu_m = 0$ and $r=n$, Equation (22) leads to the well known result; $V_m^P = 4nM^P / h_m$ [20]. Next substituting for M^P from (22) into (23) and replacing, $\psi_{mp} - \phi_m = \Delta_{m,s=3}^P$ it relates the maximum target drift to the collapse load as:

$$\psi_{mp} - \phi_{0m} = \frac{(V_P + P\phi_{0m})}{\sum_{s=1}^r (1-\mu_{m,s})} \sum_{s=1}^r \frac{\alpha(m,s)}{(1-\mu_{m,s})K_{m,s}} \quad (24)$$

The applications of group of Equations (16) through (24) have been studied in the following example.

6.1.1 Introductory example 2, ultimate load analysis

Study the nonlinear behavior of the MFUR of Example 1 of Section 5.2.4 above, compute the ultimate carrying capacity of the roof level subframe and check the adequacy of the selected section properties in terms of the specified drift ratio at incipient collapse; $\phi_P \leq 0.02$.

Solution: From example 1: $k_1 \neq k_2 \neq k_3$ then $s=3$ and $\tau_{m,s}=1$ for all s , then the sums of the stiffnesses of the beams and columns of the subject subframe at the first, second and third stages of loading can be computed as $\sum_{j=1}^{n=3} k_{4,j} = 13I/6L$ and $\sum_{j=0}^{n=3} \bar{k}_{4,j} = 6J/h$, $\sum_{j=2}^{n=3} k_{4,j} = 7I/6L$ and $\sum_{j=1}^{n=3} \bar{k}_{4,j} = 5J/h$, and $\sum_{j=3}^{n=3} k_{4,j} = 3I/6L$ and $\sum_{j=2}^{n=3} \bar{k}_{4,j} = 3J/h$ respectively. Consequently the corresponding stiffnesses of the degrading subframe, using Equation (8), become $\frac{1}{K_{4,s=1}} = \frac{h^2}{12E} \left[\frac{h}{6J} + \frac{6L}{2 \times 13I} \right] = \frac{31h^3}{936EI}$, $\frac{1}{K_{4,s=2}} = \frac{h^2}{12E} \left[\frac{h}{5J} + \frac{6L}{2 \times 7I} \right] = \frac{44h^3}{840EI}$

and $\frac{1}{K_{4,s=3}} = \frac{h^2}{12E} \left[\frac{h}{3J} + \frac{6L}{2 \times 3I} \right] = \frac{8h^3}{72EI}$ respectively. Similarly the stability quotients μ of the tree consecutive stages become; $\mu_{4,s=1} = \frac{P_4}{K_{4,s=1}h_4} = \frac{8F \times 31h^2}{936EI}$, $\mu_{4,s=2} = \frac{P_4}{K_{4,s=2}h_4} = \frac{8F \times 44h^2}{840EI}$ and $\mu_{4,s=3} = \frac{P_4}{K_{4,s=3}h_4} = \frac{8F \times 8h^2}{72EI}$ respectively. Substituting for $\mu = \frac{Fh^2}{EI}$, Equation (20) gives for $\delta_s^1 = 1$ for $s=1$ and $\delta_s^1 = 0$ for $s>1$:

$$V_{m,s=1} + 0.02F = \frac{4M^P}{h} \left[(1 - 0.2650\mu) \right] \frac{13}{6}, V_{m,s=2} = \frac{4M^P}{h} \left[\frac{3}{2} (1 - 0.4191\mu) - (1 - 0.2650\mu) \right] \frac{7}{6} \quad \text{and}$$

$$V_{m,s=3} = \frac{4M^P}{h} \left[\frac{2}{1} (1 - 0.8888\mu) - \frac{3}{2} (1 - 0.4191\mu) \right] \frac{3}{6} \text{ as the incremental lateral forces leading to the}$$

plastic collapse load $V_m^P = \frac{12M^P}{h} (1 - 0.5243\mu) - 0.02F_Y$. Equation (22) also yields:

$$V_m^P + 8F_Y \times 0.0025 = \frac{4M^P}{h_m} [3 - (0.2650 + 0.4191 + 0.8888)\mu] = \frac{12M^P}{h_m} [1 - 0.5243\mu] \quad (25)$$

Similarly, Equation (21) gives the corresponding incremental lateral displacements as:

$$\Delta_{m,s=1} = \frac{31h^3}{936EI} \times \frac{4M^P}{h} \left[\frac{1}{1} (1 - 0) \right] \frac{13}{6} = \frac{1612M^P h^2}{5616EI} [(1 - 0 \times \mu)] = 0.2870 \frac{M^P h^2}{EI} \quad (26a)$$

$$\Delta_{m,s=2} = \frac{4 \times 44M^P h^2}{840EI} \left[\frac{3}{2} - \frac{1}{1} \frac{(1 - 0.2650\mu)}{(1 - 0.4191\mu)} \right] \frac{7}{6} = 0.2444 \frac{M^P h^2}{EI} \left[1.5 - \frac{(1 - 0.2650\mu)}{(1 - 0.4191\mu)} \right] \quad (26b)$$

$$\Delta_{m,s=3} = \frac{4 \times 8M^P h^2}{72EI} \left[\frac{2}{1} - \frac{3}{2} \frac{(1 - 0.4191\mu)}{(1 - 0.8888\mu)} \right] \frac{3}{6} = 0.2222 \frac{M^P h^2}{EI} \left[2 - \frac{1.5 \times (1 - 0.4191\mu)}{(1 - 0.8888\mu)} \right] \quad (26c)$$

$$\Delta_{m,s=3}^P = 0.2870 \frac{M^P h^2}{EI} + \frac{M^P h^2}{EI} \left[0.3666 - \frac{(0.2444 - 0.0648\mu)}{(1 - 0.4191\mu)} \right] + \frac{M^P h^2}{EI} \left[0.4444 - \frac{(0.3333 - 0.1397\mu)}{(1 - 0.8888\mu)} \right]$$

$$\Delta_{m,s=3}^P = \left\{ (0.2870 + 0.3666 + 0.4444) - \left[\frac{0.2444 - 0.0648\mu}{1 - 0.4191\mu} + \frac{0.3333 - 0.1397\mu}{1 - 0.8888} \right] \right\} \frac{M^P h^2}{EI} \quad (26d)$$

For $\mu = 0$, Eq. (26) gives; $\Delta_{m,s=3}^P = 0.52 \frac{M^P h^2}{EI} = \frac{0.52Fh^2}{4EI} = \frac{7.6879Fh^2}{EI} = \frac{V}{K_{m,s=3}^P}$. It may be deduced from Equation (25) that $F_P = 12M^P / h$. Since, $F_Y = 7.5817M^P / h$, then $F_Y = 0.6318F_P$. Eq. (13) yields $K_{m,s=3}^P = \frac{F_P + 0.16F_Y}{(0.02 - 0.0925)h} = \frac{1.1011F_P}{0.0175h} = 7.6879 \frac{EI}{h^3}$ and $\mu = \frac{Fh^2}{EI} = \frac{7.6879}{62.92} = 0.1222$.

Since, $I = I_P = 8.1833Fh^2 / E > I_Y$, target displacements at collapse govern the final design.

Finally, the substitution of μ in Equations (25) and (26), results in force $F_p = 11.215 \frac{M^P}{h}$ and displacement $\Delta_{m,s=3}^P = 0.51 \frac{M^P h^2}{EI} = 22.1816 \frac{F_p h^2}{EI}$ respectively. While the proposed step by step solution is accurate, provides insight into the nonlinear response of the structure throughout the loading cycle and is well suited for spreadsheet and mechanized treatment, it is rather cumbersome and not as quick and as reliable as the modified virtual work method introduced below.

6.2 The modified virtual work method

The virtual work method of structural analysis is commonly associated with linear behavior of linear ductile systems at collapse. In this section an attempt has been made to extend the applications of the method to the solution of certain nonlinear problems. Despite its analytic elegance, the virtual work method of structural analysis cannot be utilized directly for nonlinear higher order computations. However, Equation (22) indicates that if the terms $P\phi_{i,m}$ and $(1 - \mu_{i,j})M^P = M_{ii,j}^C$ are treated as equivalent notional forces and notional capacities respectively, then Equation (22) may also be looked upon as the virtual work equation that equates the total virtual work of the external effects, including the notional forces to the total virtual work absorbed by the total internal, real as well as notional capacities. For instance, considering the uppermost story, it gives:

$$(V_p + P\phi_{0m}) \times \theta h_m = \sum_{s=1}^r M_{m,s}^C \theta \quad (27)$$

This results in, $(F_p + 8F_Y \times 0.0025)h = M_{m,1}^C + M_{m,2}^C + M_{m,3}^C = 12M^P[1 - 0.5243\mu]$ for the current problem. Equation (27) simply implies that for any frame with initial imperfections under lateral, and gravity forces, there exists an equivalent perfect, notional frame with reduced notional capacities and zero axial forces. The main advantage of the modified virtual work method is in that it is independent of the sequence of formation of the plastic hinges. And, as a matter of interest, summation (27) can be extended over the entire structure. However, it furnishes no information regarding the distorted shape of the structure at or prior to failure.

6.3 Short cut estimation of the maximum displacements at incipient collapse

In a well-controlled structure plasticity tends to set in the stiffest members first and then propagate toward the most flexible elements of the system [33-34]. And, as a result once the location of formation of the last sets of plastic hinges is known, the maximum lateral displacements of the system at incipient collapse can easily be estimated as that belonging to the last standing module prior to complete failure. The last failing module is that which contains the position of the last yielding member prior to formation of a collapse mechanism. Equation (8) can be used again to estimate the stiffness of the last or number 3 module at incipient collapse, thus:

$\frac{1}{K_{4,s=3}} = \frac{h^2}{12E} \left[\frac{h}{J} + \frac{6L}{2 \times 3I} \right] \frac{h^3}{2EI}$, which means that $\Delta_{m,s=3}^P = \frac{M^P h^2}{2(1-\mu)EI}$. Since because of the P-delta effects, $F_p = \frac{11.215M^P}{3}$ instead of $F_p = \frac{12M^P}{3}$, then $\frac{1}{K} = \frac{3h^3}{11.215 \times 2EI} = \frac{h^3}{7.4767}$ and $\mu = \frac{8F_Y}{Kh} = \frac{8Fh^2}{7.4767EI}$. Equation (13) gives $K_{m,s=3}^P = \frac{1.1011F_p}{0.0175h} = \frac{8EI}{7.4767h^3}$, therefore, $\frac{Fh^2}{EI} = 0.01701$ and $\Delta_{m,s=3}^P = 0.51 \frac{M^P h^2}{EI}$. This result is in excellent agreement with that of the long hand solution discussed above.

7. CONCLUSIONS

Bioinspiration and performance control are not new ideas. They have been explored successively for structural optimization [35-38] as well as improved performance [39]. A realistic analogy, with practical applications, between green trees and manmade moment frames has been presented. It has been argued that in order to transfer structural design knowledge from a living organism to an engineering framework, three conditions of affinity should be observed, structural applicability, functional similarity and response analogy. The basic Bioinspired design strategy, PC, was successfully utilized to design a regular moment frame (Examples 1 and 2) under lateral loading. As a first step a number of conceptual structural design similarities between trees and moment frames were established. The following bio-inspired attributes were incorporated as part of the proposed PC design strategies:

- Bioinspired structural design is based upon observed rather than expected behavior;
- Bioinspired structural design is a realistic method of approach that can lead to minimum material consumption;
- PC, as a bioinspired methodology, leads to uniform demand-capacity ratios throughout the structure;
- PC involves fail-self provisions that prevent formation of plastic hinges within the columns;
- In PC, the sequence of formation of the plastic hinges can be arranged in such a way as to prevent *premature* damage to columns of the lower stories;
- As in nature, in PC, failure mechanisms and stability conditions are enforced rather than tested;
- As in trees, members of the moment frame are made out of the same materials with varying strengths as required;
- The moment connections (beam joints) can achieve elastic-plastic response at extreme loading
- The grade beams tend to prevent the formation of plastic hinges at column feet;
- In PC, the rules of material science and applied mechanics are applied rather than investigated;
- PC induced uniform drift minimizes secondary and instability effects in regular

moment frames.

Two exact, parametric examples were provided to illustrate the applications of the conceptual design similarities between trees and manmade moment frames.

It has been shown that MFUR are ideally suited for Performance Based Elastic-Plastic Design. A number of new, exact, closed form formulae for understanding the response of MFUR were presented. The proposed methodology lends itself well to controlling the sequential response of MFUR due to monotonically increasing lateral forces. MFUR approach results in minimum weight solutions for lateral force resisting moment frames designed to perform as intended at any prescribed response stage. It was demonstrated through simple parametric examples that the proposed procedures provide useful design information that neither elastic nor plastic methods of analysis can offer on their own. Furthermore, it was shown that the sequences of formations of plastic hinges could be controlled by selecting the relative stiffness of groups of similar beams in accordance with predetermined performance objectives. The proposed methodology may be interpreted as an advanced or direct version of the commonly known pushover or lateral plastic analysis of earthquake resisting frameworks, with the difference that the pushover analysis is used for investigative purposes and does not result in direct member selection.

While bioinspiration and performance control are not new ideas, they need time and exposure before gaining consensus as mainstream methods of advancing structural design strategies.

REFERENCES

1. American Wood Council (AWC), http://cdn1.bigcommerce.com/server2500/hw84i/products2728/images/3890/wfcm_seismic__81050.1375832196.1280.1280.jpg, *Wood Frame Construction Manual Workbook: Design of Wood Frame Buildings for High Wind, Snow and Seismic Loads*, 2005, US.
2. Benyus J. *Biomimicry*, William Morrow and Company, New York, 1997.
3. Cattano C, Nikou T, Klotz L. Teaching systems: thinking and Biomimicry to civil engineering students, *Journal of Professional Issues in Engineering and Education Practice*, No. 4, **137**(2011) 176–82.
4. Ennos R. *Trees: Magnificent structures*, The Natural History Museum, London, 2001.
5. James KR, Hariots N, Peter K Ades. Mechanical stability of trees under dynamic loads, *American Journal of Botany*, No. 10, **93**(2006) 1522–30.
6. Knippersand J, Speck T. Design and construction principles in nature and architecture, *Bioinspiration and Biomimetics*, No. 1, **7**(2012).
7. Vogel S. *Cat's Paws and Catapults*, Norton paperback, 2000, US.
8. Xing D, Chen W. Systematic method of applying structural characteristics of natural organisms to mechanical structures, *Transactions of Tianjin University*, **17**(2011) 293–7.
9. AISC, (American Institute of Steel Construction) Seismic provisions for structural steel buildings, AISC, Chicago, Illinois, USA, 2005.
10. NBCC *National Building Code of Canada*, National Research Council of Canada, Ottawa, 1995.

11. Goel SC, Chao SH. *Performance Based Plastic Design*, ICC, US, 2008.
12. BS, 5950, Davies JM, Brown B. *Plastic Design to BS. 5950*, Steel Construction Institute, UK, 1996.
13. Grigorian M, Grigorian C. Performance control for seismic design of moment frames, *Journal of Constructional Steel Research*, **67**(2011) 1106-14.
14. Grigorian M, Grigorian C. Performance control: A new elastic-plastic design procedure for earthquake resisting moment frames, *Journal of Structural Engineering, ASCE*, No.6, **138**(2012) 812-21.
15. Grigorian M, Grigorian C. A new performance based design method for earthquake resisting moment frames, *Canadian Journal of Civil Engineering*, **39**(2012c) 1–11.
16. Grigorian M, Grigorian C. An overview on performance control and efficient design of lateral resisting moment frames, *International Journal of High-rise Buildings*, No. 2, **2**(2013).
17. Niklas KJ, Spatz HC. Wind-induced stresses in cherry trees: evidence against the hypothesis of constant stress levels, *Trees*, **14**(2000) 230-37.
18. Mattek C. *Trees: The Mechanical Design*, Springer, Verlag, 1991, Germany.
19. Brandt A. *Criteria and Methods of Structural Optimization*, Kluwer Academic publications, US, 1987.
20. Grigorian M, Grigorian C. An introduction to the methodology of earthquake resistant structures of uniform response, *Buildings*, **2**(2012) 107-25.
21. Grigorian M. An introduction to performance control for moment frames of uniform response under lateral loading, *Asian Journal of Civil Engineering*, No.1, **14**(2013) 123-43.
22. Grigorian M. On the efficient design of earthquake resistant moment frames, *Asian Journal of Civil Engineering*, No. 2, **14**(2013b) 319-38.
23. Surovek AE, Camotim DA, Hajjar J, Teh L, White DW, Ziemian RD. Direct second order analysis for the design of steel structures, *Proceeding of ASCE Structures Congress*, St. Louis, MO, US, 2006.
24. Schafer D, Eichler B, Amlung L. *Modern plastic design for steel structures*, EU Publications, LUX, 2010.
25. Naeim F. *The Seismic Design Handbook*, Kluwer Academic Publishers, U.S, 2001.
26. Bozorgnia Y, Bertero VV. *Earthquake Engineering*, CRC Press, U.S, 2004.
27. Hamburger RO, Krawinkler H, Malle, JO. Seismic design of steel special moment frames: a guide for practicing engineers, *NEHRP Seismic Design Technical Brief*, No. 2, 2009.
28. Grigorian M, Grigorian C. Drift Control for multistory moment frames under lateral loading, *International Journal of High-Rise Buildings*, No 4, **2**(2013) 1-11.
29. Faulks J. Minimum weight design and the theory of plastic collapse, *Quarterly of Applied Mathematics*, **10**(1954) 347.
30. Faulks J. The minimum weight design of moment frames, *Proceedings of the Royal Society A*, **223**(1954) 482-94.
31. Neal BG. *The plastic methods of structural analysis*, Chapman & Hall Ltd. UK, 1963.
32. Nethercot DA. *Limit State Design of Structural Steelwork*, Spon Press, UK, 2001.
33. Heyman J. On the estimation of deflections in elastic plastic frames, *Proceedings, Institution of Civil Engineering*, **19**(1961) 89.
34. Grigorian M, Grigorian C. Lateral displacements of moment frames at incipient

- collapse, *Journal of Engineering Structures*, **44**(2012) 174–85.
35. Kaveh A, Farahmand Azar B, Hadidi A, Rezazadeh Sorochi F, Talatahari S. Performance-based seismic design of steel frames using ant colony optimization, *Journal of Constructional Steel Research*, No. 4, **66**(2010) 566-74.
36. Kaveh A, Khanlari K. Collapse load factor of planar frames using a modified Genetic algorithm, *Communications on Numerical Methods in Engineering*, **20**(2004) 911-25.
37. Kaveh A, Talatahari S. An improved ant colony optimization for design of steel frames, *Engineering Structures*, **32**(2010) 864-73.
38. Kaveh A, Jahanshahi M. Plastic limit analysis of frames using ant colony systems, *Computers and Structures*, **86**(2008) 1152-63.
39. Grigorian M. Bionics and theory of structures-design methodology transfer from trees to moment frames, *Journal of Bionic Engineering*, 2014 (in press).

APPENDIX 1- EQUIVALENT WEIGHT SYSTEMS FORSIMPLY SUPPORTEDBEAMS

The simply supported beam of 5(a), is assumed to be equivalent in nature to two cantilevers with similar or varying cross sections under similar loading. Therefore, the total self weight can be computed as:

$$G_b \leq G_a \text{ and } G_d \leq G_c \quad (28)$$

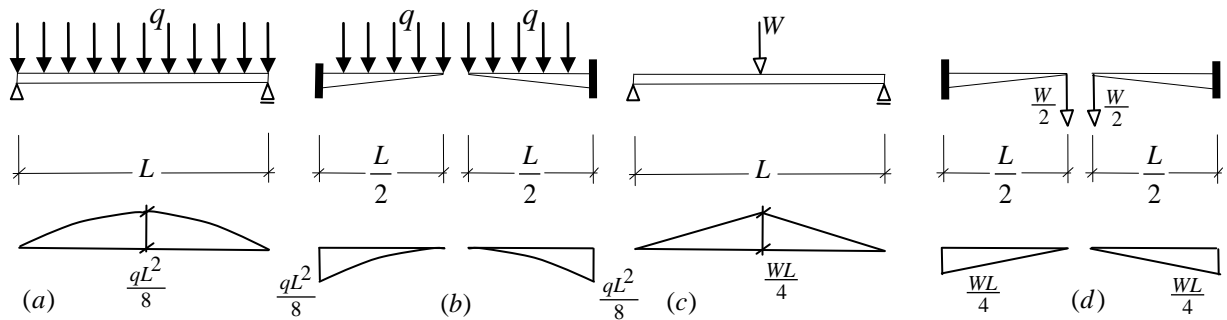


Figure 5. (a) Simply supported beam under uniform loading, (b) Twin weight improved cantilevered beams under uniform loading, (c) Simply supported beam under central point load, (d) Twin, equivalent, weight improved cantilevered beams under concentrated end loads

$$\text{Where, } G_a = \gamma M_a^P L = \frac{\gamma q L^3}{8} \text{ and } G_b = 2\gamma \int_0^{\frac{L}{2}} M_b(x) dx = 2\gamma \int_0^{\frac{L}{2}} \left[\frac{qx^2}{2} \right] dx = \frac{\gamma q L^3}{24} \quad (29)$$

$$G_c = \gamma M_c^P L = \frac{\gamma W L^2}{4} \text{ and } G_d = 2\gamma \int_0^{\frac{L}{2}} M_d(x) dx = 2\gamma \int_0^{\frac{L}{2}} \left[\frac{Wx}{2} \right] dx = \frac{\gamma W L^2}{8} \quad (30)$$

APPENDIX 2- SUBFRAME STIFFNESS IN TERMS OF TARGET AND INITIAL DRIFT RATIOS

Equation (10) clearly expresses the effects of P and φ_0 on the deformations of the subject subframe. However, if the subframe stiffness K_i needs to be controlled, then it must be defined in terms of the total target drift ratio ψ_i discussed above. By definition:

$$\psi_i = \phi_i + \varphi_{0i} = \frac{V_i}{(1 - \mu_i)K_i h_i} + \frac{\mu \varphi_{0i}}{(1 - \mu_i)} + \varphi_{0i} \quad (31)$$

Equation (31) may be expanded as;

$$\psi_i = \phi_i + \varphi_{0i} = \frac{\phi_i}{(1 - \mu_i)} + \frac{\mu \varphi_{0i}}{(1 - \mu_i)} + \varphi_{0i} = \frac{\phi_i + \varphi_{0i}}{(1 - \mu_i)} \quad (32)$$

In other words, $\psi(1 - \mu_i) = \phi_i + \varphi_{0i}$, $\psi_i(1 - \frac{P_i}{K_i h_i}) = \frac{V_i}{K_i h_i} + \varphi_{0i}$ or $\psi_i - \frac{\psi_i P_i}{K_i h_i} = \frac{V_i}{K_i h_i} + \varphi_{0i}$ which gives,

$$\text{upon simplification; } K_i = \frac{V_i + \psi_i P_i}{(\psi_i - \varphi_{0i}) h_i} \quad (33)$$

APPENDIX 3- MOMENTS OF BEAMS, BAY # 1 OF EXAMPLE 1 AT FIRST YIELD

The elastic moments of the beams of the subframes of bay 1 can be computed using Equation (15) as:

$$M_{4,1} = \frac{(V_4 + P_4 \varphi_4) h_4 k_{4,j}}{4(1 - \mu_4) \sum_{j=1}^n k_{4,j}} = \frac{(F + 0.01 \times 8F)}{4 \times 0.9444 \times \frac{13}{6L}} = \frac{6.48Fh}{49.1111} = 0.1319Fh = M^P \quad (34a)$$

$$M_{3,1} = \frac{(V_3 + P_3 \varphi_3) h_3 k_{3,j}}{4(1 - \mu_3) \sum_{j=1}^n k_{3,j}} = \frac{(1.8182F + 0.01 \times 16F)}{4 \times 0.9393 \times \frac{13}{6L}} = \frac{11.8692Fh}{48.8436} = 0.2430Fh = 1.8423M^P \quad (34b)$$

$$M_{2,1} = \frac{(V_2 + P_2 \varphi_2) h_2 k_{2,j}}{4(1 - \mu_2) \sum_{j=1}^n k_{2,j}} = \frac{(2.4092F + 0.01 \times 24F)}{4 \times 0.9321 \times \frac{13}{6L}} = \frac{15.8952Fh}{48.4692} = 0.3279Fh = 2.4860M^P \quad (34c)$$

$$M_{1,1} = \frac{(V_1 + P_1 \varphi_1) h_1 k_{1,j}}{4(1 - \mu_1) \sum_{j=1}^n k_{1,j}} = \frac{(2.7273F + 0.01 \times 32F)}{4 \times 0.9212 \times \frac{13}{6L}} = \frac{18.2838Fh}{47.90242} = 0.3817Fh = 2.9340M^P \quad (34d)$$

The elastic moments of the remaining beams of the roof level subframe can also be computed as:

$$M_{4,2} = \frac{0.132Fh}{1.5} = 0.0879Fh \text{ and } M_{4,3} = \frac{0.132Fh}{2} = 0.0659Fh \quad (35)$$

APPENDIX 4- STIFFNESSES OF SUBFRAMES OF EXAMPLE 1 AT FIRST YIELD

$$\frac{I}{K_4} = \frac{h^2}{12E} \left[\frac{h}{6J} + \frac{6L}{2 \times 13I} \right] = \frac{31h^3}{936EI}, \quad K_4 = \frac{144F}{h}, \quad I_{4,1} = J_{4,0} = 4.77Fh^2 / E = I \quad (36a)$$

$$\frac{I}{K_3} = \frac{1.5625h^2}{12E} \left[\frac{1.25h}{6J_3} + \frac{3L}{13I_3} \right] = \frac{53.52h^3}{936EI}, \quad K_3 = \frac{211F}{h}, \quad (36b)$$

$$I_{3,1} = J_{3,0} = 12.07Fh^2 / E = 2.53I$$

$$\frac{I}{K_2} = \frac{2.2500h^2}{12E} \left[\frac{1.5h}{6J_3} + \frac{3L}{13I_3} \right] = \frac{84.375h^3}{936EI}, \quad K_2 = \frac{235.48F}{h}, \quad (36c)$$

$$I_{2,1} = J_{2,0} = 21.23Fh^2 / E = 4.45I$$

$$\frac{I}{K_1} = \frac{3.0625h^2}{12E} \left[\frac{1.75h}{6J_3} + \frac{3L}{13I_3} \right] = \frac{124.797h^3}{936EI}, \quad K_1 = \frac{232.18F}{h}, \quad (36d)$$

$$I_{1,1} = 30.96Fh^2 / E = 6.49I$$